Observation of quasi-two-dimensional superconductivity at the EuO-$BaBiO_3$ interface

Weiliang Qiao,[1,*] Jiali Zhao,[2,*] Yuxiao Chen,[1] Shenggen Cao,[2,3] Wenyu Xing,[1] Ranran Cai,[1] Liangliang Guo,[1] Tian Qian,[2] X. C. Xie,[1,4,5] and Wei Han[1,†]

[1]*International Center for Quantum Materials, School of Physics, Peking University, Beijing 100871, People's Republic of China*
[2]*Beijing National Laboratory for Condensed Matter Physics, Institute of Physics, Chinese Academy of Sciences, Beijing 100190, China*
[3]*School of Physical Sciences, University of Chinese Academy of Sciences, Beijing 101408, China*
[4]*Institute for Nanoelectronic Devices and Quantum Computing, Fudan University, Shanghai 200433, People's Republic of China*
[5]*Hefei National Laboratory, Hefei 230088, People's Republic of China*

(Received 14 November 2022; revised 24 July 2023; accepted 24 January 2024; published 13 February 2024)

The recent discoveries of superconducting oxide interfaces provide new platforms to explore the exotic superconducting properties in the two-dimensional (2D) regime. In this paper, we report the observation of quasi-2D superconductivity at the EuO/$BaBiO_3$ (001) interface with the superconducting transition temperature of ~3.5 K. The current-voltage characteristics reveal the signature of a Berezinski-Kosterlitz-Thouless transition, which indicates the existence of quasi-2D superconducting interface. Furthermore, the quasi-2D nature is also supported by the temperature- and angle-dependent upper critical fields. The realization of quasi-2D superconductivity in the $BaBiO_3$ heterostructures could be useful for the emergent research field of superconducting oxide interfaces.

DOI: 10.1103/PhysRevB.109.054509

I. INTRODUCTION

In the last few decades, two-dimensional (2D) superconductivity has been one of the most interesting research fields in condensed-matter physics and materials science. The reduced dimension of superconductivity to 2D leads to progress of many exciting quantum phenomena, including transition-temperature oscillations [1], Berezinski-Kosterlitz-Thouless (BKT) transition [2], and quantum-phase transitions [3], etc. Among these 2D superconducting systems, oxide interfaces are particularly interesting since the superconductivity is buried between two *insulating* oxides. The first discovery of superconducting interface was made in the $SrTiO_3$ heterostructures when a thin $LaAlO_3$ layer was grown on the $SrTiO_3$ substrate [2,4]. Since then, large efforts have been spent to enhance the superconducting critical temperature (T_C) of the interface states. Recently, a T_C of ~2 K has been achieved in the EuO (or $LaAlO_3$)/$KTaO_3$(111) heterostructures [5–7], which is much higher compared to that in the $SrTiO_3$ - based heterostructures. Besides, the interface engineering offers a promising route to construct superconducting interface states that do not exist in nature but exhibit unconventional physical properties [8–14]. The search for higher-T_C superconducting interface states has been a competitive and active research direction.

$BaBiO_3$ is a perovskite which has a monoclinic crystalline structure with distortion of octahedral BiO_6 [15]. Previous reports have shown that hole-doped $BaBiO_3$ is superconducting with relatively high T_C in the bulk materials. These samples include lead-doped $BaBiO_3$ ($BaBi_{1-x}Pb_xO_3$) [16,17] and potassium-doped $BaBiO_3$ ($Ba_{1-x}K_xBiO_3$) [18], etc., and the T_C could be as high as ~30 K [19]. Furthermore, superconductivity was observed in the $BaPbO_3$/$BaBiO_3$ heterostructures with carriers still in the hole-doped regime [20]. Following the well-known superconducting phase diagrams of cuprates and iron-based superconductors [21,22], one would expect electron doping could also lead to superconductivity in $BaBiO_3$. However, the electron-doped superconductivity in $BaBiO_3$ systems has not been realized yet.

In this paper, we report the discovery of the quasi-2D superconductivity (SC) at the interface of the EuO/$BaBiO_3$ (001) heterostructures with a T_C up to ~3.51 K. This T_C is much higher compared to those in the $SrTiO_3$- and $KTaO_3$-based heterostructures. The current (I)-voltage (V) indicates a BKT phase transition that manifests the quasi-2D nature of the superconductivity. Magnetoresistance studies of the critical magnetic fields are investigated using Tinkham's analysis and Ginzburg-Landau (GL) theory, which further support the existence of a quasi-2D superconducting interface. Our results demonstrate that interface engineering could be a promising way to construct quasi-2D superconductors.

II. EXPERIMENT

Figure 1(a) shows the schematic of the EuO/$BaBiO_3$ (001) heterostructures. The $BaBiO_3$ thin films of ~25 nm were deposited on TiO_2-terminated $SrTiO_3$ (001) substrates at 500° C with oxygen partial pressures of 10 Pa in a pulsed laser deposition system using a KrF excimer laser (1.2 J/cm^2, 248 nm, 2 Hz). After the growth, the samples were cooled to room temperature under the same oxygen pressure as used during the growth. The epitaxial growth of $BaBiO_3$ thin films has been confirmed by *in situ* reflective high-energy electron diffraction (RHEED) [Fig. 1(b)] and high-resolution x-ray-diffraction (XRD) characterizations [Fig. 1(c)]. After the

*These authors contributed equally to this work.
†Corresponding author: weihan@pku.edu.cn

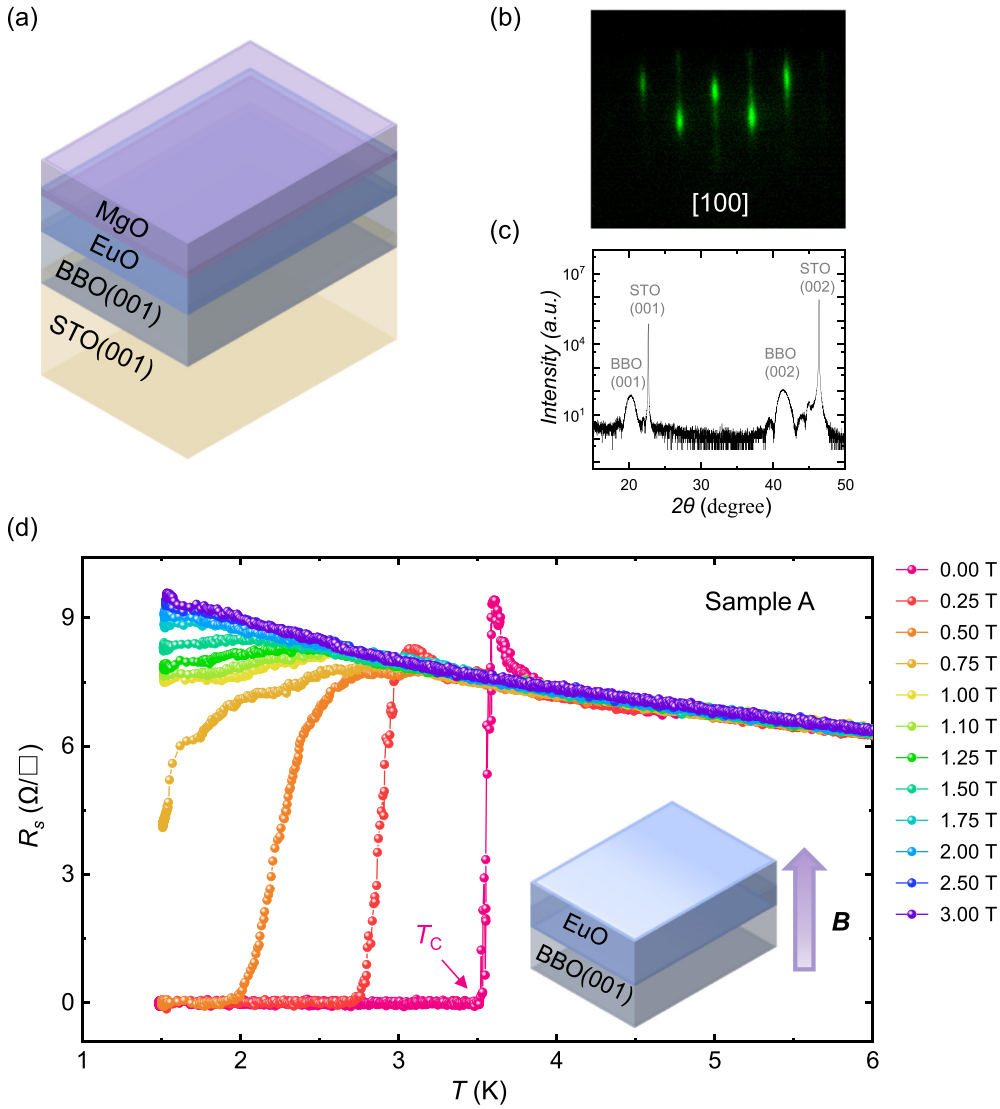

FIG. 1. The schematic and characterization of superconducting $EuO/BaBiO_3$ (001) interface. (a) Schematic of $EuO/BaBiO_3$ heterostructures. The $BaBiO_3$ film was grown on the $SrTiO_3$ (001) substrate and the ∼5-nm-thick MgO was used to protect EuO from degradation during measurement. (b), (c) RHEED and XRD characterization of the $BaBiO_3$ film. BBO and STO stand for $BaBiO_3$ and $SrTiO_3$. (c) The temperature dependence of the sheet resistance of $EuO/BaBiO_3$ (Sample A) under various out-of-plane magnetic fields. T_C is determined as the zero-resistance temperature.

growth of $BaBiO_3$ thin films, the wafers were loaded into an oxide molecular-beam epitaxy chamber (MBE-Komponenten GmbH; Octoplus 400) with a base pressure lower than 5×10^{-10} mbar for the growth of EuO thin films. Prior to the EuO growth, the $BaBiO_3$ thin films were insulating. There were two steps of EuO growth with the $BaBaO_3/SrTiO_3$ wafer heated at 500° C, including the deposition Eu from a low-temperature thermal effusion cell in the pressure of $\sim 5 \times 10^{-9}$ mbar for ∼20 min and with oxygen partial pressure of $\sim 1 \times 10^{-9}$ mbar for ∼20 min. After the EuO growth, a thin MgO layer (∼5 nm) was deposited via e-beam evaporation *in situ* to protect the EuO films from degradation. The growth conditions of EuO were similar to our previous work on superconducting $EuO/KTaO_3$ (111) interfaces [12,14].

The transport properties of $EuO/BaBiO_3$ heterostructures were measured using the van der Pauw geometries with Al conducting wires bonded at the four corners for contacts. The electrical measurements were conducted at various temperatures in a physical properties measurement system (PPMS, Quantum Design). For the sheet resistance (R_s) measurement as a function of temperature (T) and magnetic field (B), a low-frequency ac current $I = 10\,\mu A$ ($f = 7$ Hz) was applied using a current source (Keithley 6221), and the voltage was measured using a lock-in amplifier (Stanford Research SR830). For the critical current measurements, the dc technique was conducted using a voltage-current source (Keithley 2400) and a multimeter (Keithley 2002) with a DC current from 0 to ∼0.6 mA.

III. RESULTS AND DISCUSSION

Figure 1(d) shows the temperature-dependent R_s under various magnetic fields (B) measured on a typical $EuO/BaBiO_3$ interface (sample A). At $B = 0$ T, a sharp transition to zero

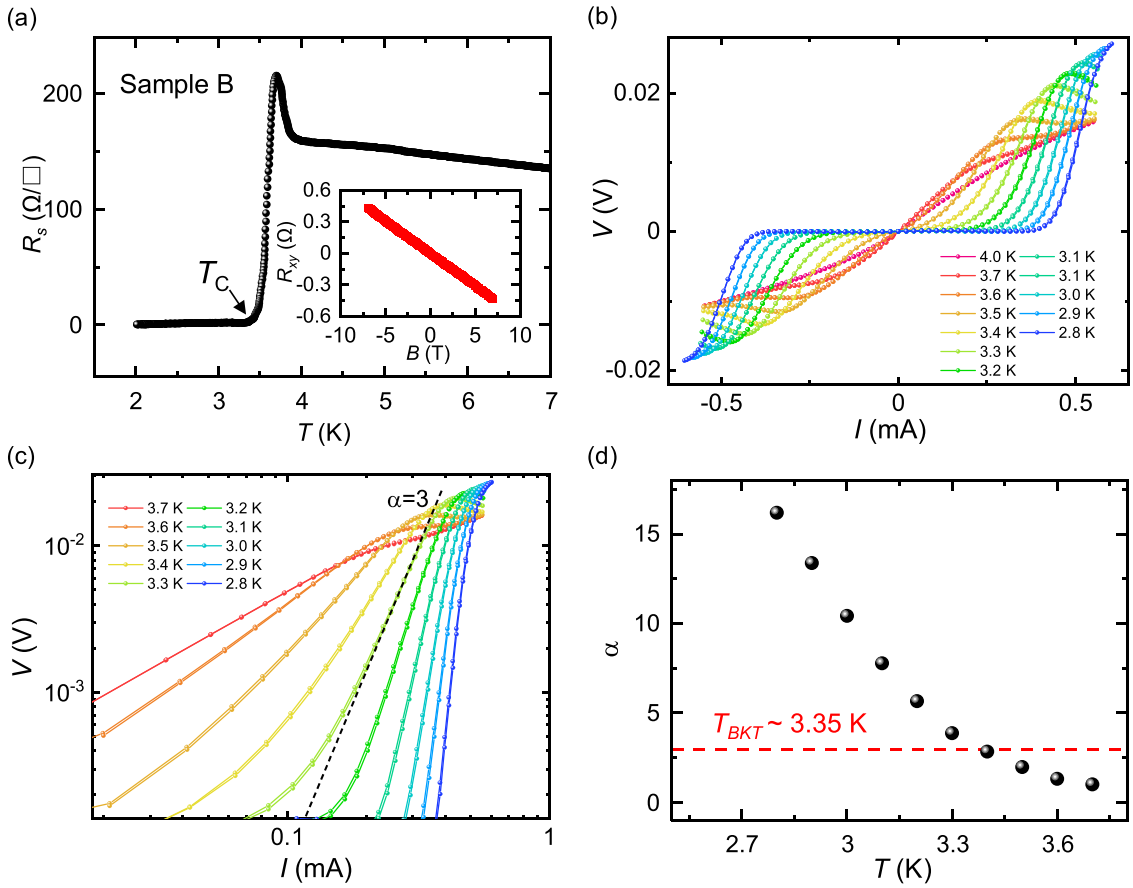

FIG. 2. The Berezinski-Kosterlitz-Thouless (BKT) transition of superconducting EuO/$BaBiO_3$ (001) interface. (a) The temperature dependence of the sheet resistance of the EuO/$BaBiO_3$ (001) interface (sample B). Inset: Hall resistance R_{xy} vs B, which shows the electron-type carrier density of $n_s = 1.01 \times 10^{16}$ cm^{-2}. (b) The current-voltage (I-V) curves measured at T from 2.8 to 4.0 K. (c) Log-log plot of I-V curves at various temperatures, where the black dashed line presents the curve with power coefficient $\alpha = 3$. (d) The BKT transition temperature (T_{BKT}) determined from power coefficient α vs T relationship.

resistance is observed, manifesting the superconducting phase transition with T_C of ~3.51 K. The resistance peak right above the critical temperature may be due to the granular nature of superconducting interface [23,24]. Since both $BaBiO_3$ films and EuO thin films are insulating [25,26], the only possible superconducting regime is the interface between $BaBiO_3$ and EuO. This feature is similar to previous oxide interfaces of $LaAlO_3/SrTiO_3$ and EuO ($LaAlO_3$)/$KTaO_3$(111) [2,5]. The R_s vs T curves show a superconductor-insulator transition (SIT) as the out-of-plane magnetic field increases up to 3 T, as shown in Fig. 1(d). The observed zero resistance below T_C and magnetic field-induced SIT are compelling evidence for the superconducting interfaces in the EuO/$BaBiO_3$ heterostructures.

To further confirm the superconducting interface, the detailed superconducting properties are characterized from another typical EuO/$BaBiO_3$ sample (sample B). Figure 2(a) shows R_s vs T curve, with T_C of ~3.43 K. The EuO/$BaBiO_3$ interface shows electron-doping properties characterized by negative slope of the Hall voltage measurement at $T =$ 10 K [inset of Fig. 2(a)], and the calculated sheet-carrier density is 1.01×10^{16} cm^{-2}. Very interestingly, this result, together with previous results on the hole-doped $BaBiO_3$ bulk materials, are strong evidence that both electron- and hole-doped $BaBiO_3$ can be superconducting. Thus, the superconductivity in $BaBiO_3$ samples exhibits a similar superconducting phase diagram as cuprates and iron-based superconductors [21,22]. However, the origin of this carrier density is still unknown at the present stage and further studies are needed.

Figure 2(b) shows the measured current (I)-voltage (V) curves at T from 2.8 to 4.0 K. A finite voltage can be detected above the critical current (I_C), which is expected for typical superconducting materials. The I-V curves are plotted in log-log form in Fig. 2(c). At low temperatures, the power coefficient (α) of $V \propto I^{\alpha}$ is larger than 1, and these I-V characteristics can be attributed to the current-driven unbinding vortex-antivortex pairs [27]. The existence of binding vortex-antivortex pairs helps to stabilize 2D SC [28,29]. As the temperature increases, the density of vortex-antivortex pairs will increase and begin to unbind at the BKT temperature [30], denoted as T_{BKT}. T_{BKT} is obtained to be ~3.35 K [see Fig. 4(c)], which is marked by the red dashed line with the power coefficient $\alpha = 3$. Moreover, the R_s vs T curve can be well fitted by the Halperin-Nelson formula [31] (Fig. S2 [32]), and T_{BKT} is ~3.31 K, consistent with the analysis of

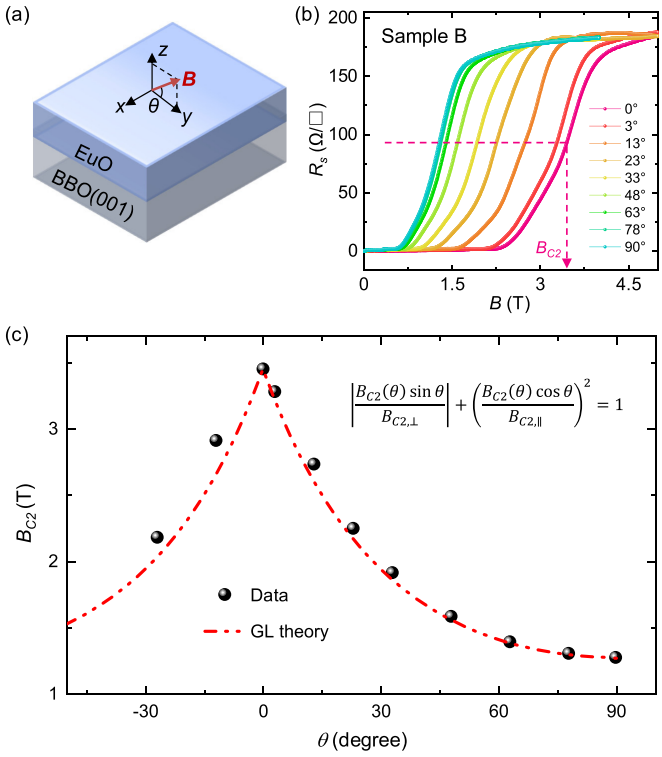

FIG. 3. The quasi-two-dimensional feature of the superconducting $EuO/BaBiO_3$ (001) interface. (a) The schematic of measurement geometry under external magnetic field from parallel to perpendicular directions. (b) The sheet resistance as a function of magnetic field at $T = 2$ K under various magnetic field angles from 0° to 90°. The upper critical field is determined as the field where the resistance is 50% of the normal-state resistance, as illustrated by the dashed purple line. (c) The angle dependence of the upper critical field. The red dashed line represents Tinkham's analysis for the 2D superconductor in the Ginzburg-Landau (GL) regime based on Eq. (1).

temperature-dependent *I-V* curves. All these characteristics are consistent with a BKT transition, indicating that the interface in $EuO/BaBiO_3$ heterostructures is a quasi-2D superconductor. To fully support this conclusion, further investigations are needed.

To further investigate the quasi-2D properties of the superconducting $EuO/BaBiO_3$ interface, measurements of the angle-dependent critical magnetic fields are performed, as illustrated in Fig. 3(a). As the magnetic field angle varies, the profile of R_s vs B changes significantly at $T = 2$ K [Fig. 3(b)]. Under in-plane direction, the critical magnetic field is much larger compared to that under the out-of-plane direction. Quantitatively, we analyze the upper critical fields following previous reports [6,11,14], where the upper critical fields are defined as the magnetic field under which the resistances are half of their normal-state values [dashed line in Fig. 3(b)]. The angle-dependent critical magnetic fields are summarized in Fig. 3(c). The out-of-plane critical magnetic field is ∼1.3 T, which is significantly smaller compared to the in-plane critical magnetic field of ∼3.5 T. This behavior is typical for quasi-2D superconductors [20,33,34]. Following Tinkham's analysis [35], the angle-dependent critical field can be described by Eq. (1),

$$\left|\frac{B_{C2}(\theta)\sin\theta}{B_{C2,\perp}}\right| + \left(\frac{B_{C2}(\theta)\cos\theta}{B_{C2,\parallel}}\right)^2 = 1, \tag{1}$$

where $B_{C2}(\theta)$, $B_{C2,\parallel}$, and $B_{C2,\perp}$ are the upper critical magnetic fields corresponding to angles θ, 0°, and 90°, respectively. As shown as the red dashed line in Fig. 3(c), the experimental results and the simulation based on Eq. (1) agree well with each other. These angle-dependent critical-field results further support the quasi-2D nature of superconductivity $EuO/BaBiO_3$ interface.

Figures 4(a) and 4(b) show the R_s vs B curves under the out-of-plane and in-plane magnetic fields at various temperatures from $T = 1.7$ to 3.4 K. As temperature increases, the upper critical field decreases for both in-plane and out-of-plane magnetic fields. The temperature-dependent perpendicular upper critical field $B_{C2,\perp}(T)$ is summarized in Fig. 4(c). The linearity of $B_{C2,\perp}(T)$ can be well fitted by GL theory for superconducting thin films [35], following Eq. (2):

$$B_{C2,\perp}(T) = \frac{\Phi_0\left(1 - \frac{T}{T_C}\right)}{2\pi\xi_{GL}^2}, \tag{2}$$

where Φ_0 and ξ_{GL} are the flux quantum and Ginzburg-Landau coherence length at $T = 0$ K, respectively. The best linear fit gives $\xi_{GL} \sim 10.6$ nm, as shown by the black dashed line in Fig. 4(c). Figure 4(d) shows the temperature-dependent parallel upper critical field $B_{C2,\parallel}(T)$. According to Tinkham's analysis for 2D superconductor [35], $B_{C2,\parallel}(T)$ has square-root dependence on T, as expressed in Eq.(3) below:

$$B_{C2,\parallel}(T) = \frac{\Phi_0\left[12\left(1 - \frac{T}{T_C}\right)\right]^{1/2}}{2\pi d\xi_{GL}}, \tag{3}$$

where d stands for the thickness of superconducting film. Using ξ_{GL} obtained from the linear fitting of $B_{C2,\perp}$ (T), d is estimated to be ∼20.9 nm based on Eq. (3) [the dashed line in Fig. 4(d)]. It is noted that the ξ_{GL} fitting from $B_{C2,\perp}(T)$ results is ∼10.6 nm, which is smaller than d of ∼20.9 nm. One possible reason for this might be related to the anisotropy of the in-plane and out-of-plane coherent lengths, i.e., $\xi_{GL,\perp} \neq \xi_{GL,\parallel}$. Nevertheless, the temperature-dependent *I-V* and upper critical-field results all support the quasi-2D nature of the superconducting $EuO/BaBiO_3$ (001) interfaces.

IV. CONCLUSION

In summary, a quasi-2D superconductivity at the $EuO/BaBiO_3$ interface is constructed using MBE and pulsed laser deposition. The achieved T_C is up to ∼3.5 K, which is much higher compared to previous results in the $SrTiO_3$- and $KTaO_3$-based heterostructures [2,4,5,13]. The *I-V* curves indicate a BKT phase transition for the quasi-2D superconducting interface. Furthermore, the angle- and temperature-dependent critical fields also show the quasi-two-dimensional nature of interfacial superconductivity. Our results could pave the way for future investigation of 2D superconductivity in the $BaBiO_3$-based heterostructures.

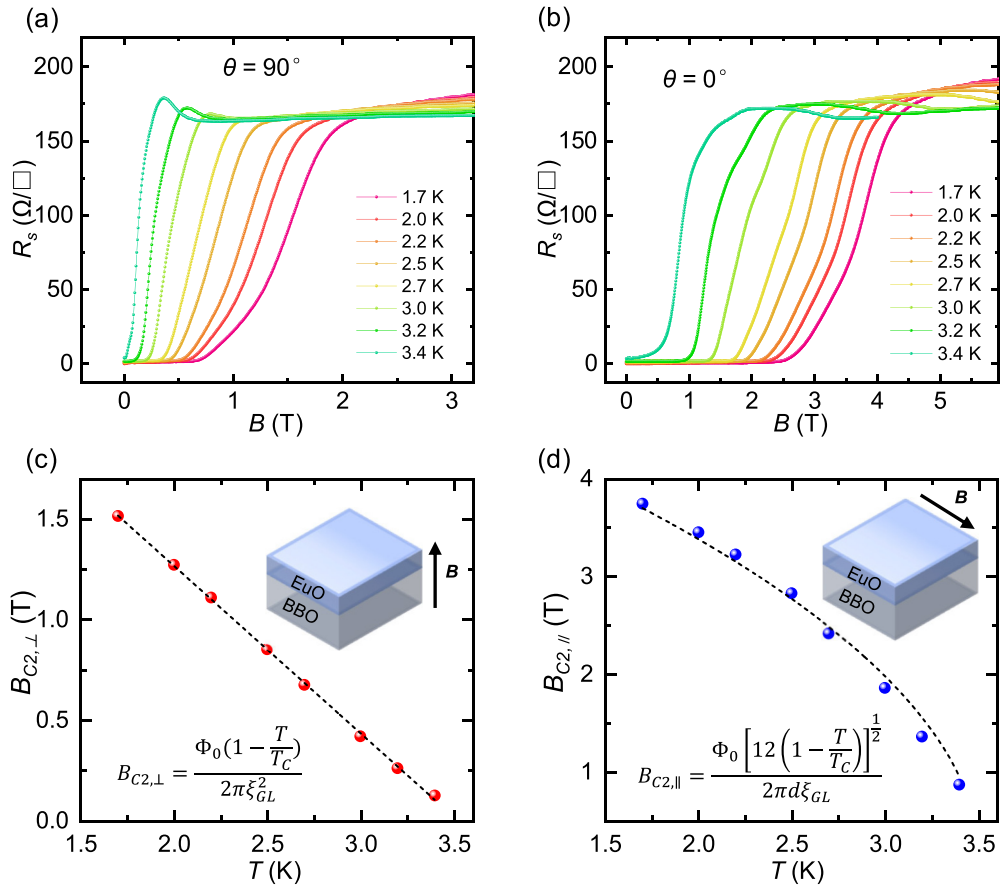

FIG. 4. The in-plane and out-of-plane upper critical fields of the superconducting EuO/$BaBiO_3$ (001) interface. (a), (b) The R_s vs B curves of sample B at various temperatures under out-of-plane and in-plane upper critical fields, respectively. (c), (d) The out-of-plane and in-plane upper critical fields as a function of temperature. The black dashed lines represent fitting curves following the GL theory. Insets show the measurement geometry and fitting equations.

ACKNOWLEDGMENTS

This work is supported by the financial support from National Basic Research Programs of China (Grants No. 2019YFA0308401 and No. 2022YFA1405100), National Natural Science Foundation of China (Grants No. 11974025 and No. 12005252), Strategic Priority Research Program of the Chinese Academy of Sciences (Grant No. XDB28000000), and National Key R&D Program of China (Grant No. 2023YFA1406100). A portion of this work was carried out at the Synergetic Extreme Condition User Facility (SECUF).

[1] B. G. Orr, H. M. Jaeger, and A. M. Goldman, Transition-temperature oscillations in thin superconducting films, Phys. Rev. Lett. **53**, 2046 (1984).

[2] N. Reyren, S. Thiel, A. D. Caviglia, L. F. Kourkoutis, G. Hammerl, C. Richter, C. W. Schneider, T. Kopp, A.-S. Rüetschi, D. Jaccard, M. Gabay, D. A. Muller, J.-M. Triscone, and J. Mannhart, Superconducting interfaces between insulating oxides, Science **317**, 1196 (2007).

[3] Y. Saito, T. Nojima, and Y. Iwasa, Quantum phase transitions in highly crystalline two-dimensional superconductors, Nat. Commun. **9**, 778 (2018).

[4] A. D. Caviglia, S. Gariglio, N. Reyren, D. Jaccard, T. Schneider, M. Gabay, S. Thiel, G. Hammerl, J. Mannhart, and J. M. Triscone, Electric field control of the $LaAlO_3/SrTiO_3$ interface ground state, Nature (London) **456**, 624 (2008).

[5] C. Liu, X. Yan, D. Jin, Y. Ma, H.-W. Hsiao, Y. Lin, T. M. Bretz-Sullivan, X. Zhou, J. Pearson, B. Fisher, J. S. Jiang, W. Han, J.-M. Zuo, J. Wen, D. D. Fong, J. Sun, H. Zhou, and A. Bhattacharya, Two-dimensional superconductivity and anisotropic transport at $KTaO_3$ (111) interfaces, Science **371**, 716 (2021).

[6] Z. Chen, Z. Liu, Y. Sun, X. Chen, Y. Liu, H. Zhang, H. Li, M. Zhang, S. Hong, T. Ren, C. Zhang, H. Tian, Y. Zhou, J. Sun, and Y. Xie, Two-dimensional superconductivity at the $LaAlO_3/KTaO_3$(110) heterointerface, Phys. Rev. Lett. **126**, 026802 (2021).

[7] X. Hua, F. Meng, Z. Huang, Z. Li, S. Wang, B. Ge, Z. Xiang, and X. Chen, Tunable two-dimensional superconductivity and spin-orbit coupling at the EuO/$KTaO_3$(110) interface, npj Quantum Mater. **7**, 97 (2022).

[8] H. Y. Hwang, Y. Iwasa, M. Kawasaki, B. Keimer, N. Nagaosa, and Y. Tokura, Emergent phenomena at oxide interfaces, Nat. Mater. **11**, 103 (2012).

[9] C. Richter, H. Boschker, W. Dietsche, E. Fillis-Tsirakis, R. Jany, F. Loder, L. F. Kourkoutis, D. A. Muller, J. R. Kirtley, C. W. Schneider, and J. Mannhart, Interface superconductor with gap behaviour like a high-temperature superconductor, Nature (London) **502**, 528 (2013).

[10] G. Cheng, M. Tomczyk, S. Lu, J. P. Veazey, M. Huang, P. Irvin, S. Ryu, H. Lee, C. B. Eom, C. S. Hellberg, and J. Levy, Electron pairing without superconductivity, Nature (London) **521**, 196 (2015).

[11] S. C. Shen, B. B. Chen, H. X. Xue, G. Cao, C. J. Li, X. X. Wang, Y. P. Hong, G. P. Guo, R. F. Dou, C. M. Xiong, L. He, and J. C. Nie, Gate dependence of upper critical field in superconducting (110) $LaAlO_3/SrTiO_3$ interface, Sci. Rep. **6**, 28379 (2016).

[12] Y. Ma, J. Niu, W. Xing, Y. Yao, R. Cai, J. Sun, X. C. Xie, X. Lin, and W. Han, Superconductor-metal quantum transition at the $EuO/KTaO_3$ interface, Chin. Phys. Lett. **37**, 117401 (2020).

[13] Z. Chen, Y. Liu, H. Zhang, Z. Liu, H. Tian, Y. Sun, M. Zhang, Y. Zhou, J. Sun, and Y. Xie, Electric field control of superconductivity at the $LaAlO_3/KTaO_3(111)$ interface, Science **372**, 721 (2021).

[14] W. Qiao, Y. Ma, J. Yan, W. Xing, Y. Yao, R. Cai, B. Li, R. Xiong, X. C. Xie, X. Lin, and W. Han, Gate tunability of the superconducting state at the $EuO/KTaO_3(111)$ interface, Phys. Rev. B **104**, 184505 (2021).

[15] D. E. Cox and A. W. Sleight, Crystal structure of $Ba_2Bi^{3+}Bi^{5+}O_6$, Solid State Commun. **19**, 969 (1976).

[16] A. W. Sleight, J. L. Gillson, and P. E. Bierstedt, High-temperature superconductivity in the $BaPb_{1-x}Bi_xO_3$ systems, Solid State Commun. **17**, 27 (1975).

[17] P. Giraldo-Gallo, H. Lee, Y. Zhang, M. J. Kramer, M. R. Beasley, T. H. Geballe, and I. R. Fisher, Field-tuned superconductor-insulator transition in $BaPb_{1-x}Bi_xO_3$, Phys. Rev. B **85**, 174503 (2012).

[18] A. W. Sleight, Bismuthates: $BaBiO_3$ and related superconducting phases, Physica C (Amsterdam, Neth.) **514**, 152 (2015).

[19] R. J. Cava, B. Batlogg, J. J. Krajewski, R. Farrow, L. W. Rupp, A. E. White, K. Short, W. F. Peck, and T. Kometani, Superconductivity near 30 K without copper: The $Ba_{0.6}K_{0.4}BiO_3$ perovskite, Nature (London) **332**, 814 (1988).

[20] B. Meir, S. Gorol, T. Kopp, and G. Hammerl, Observation of two-dimensional superconductivity in bilayers of $BaBiO_3$ and $BaPbO_3$, Phys. Rev. B **96**, 100507(R) (2017).

[21] X. Zhou, W.-S. Lee, M. Imada, N. Trivedi, P. Phillips, H.-Y. Kee, P. Törmä, and M. Eremets, High-temperature superconductivity, Nat. Rev. Phys. **3**, 462 (2021).

[22] I. I. Mazin, Superconductivity gets an iron boost, Nature (London) **464**, 183 (2010).

[23] C. Christiansen, L. M. Hernandez, and A. M. Goldman, Evidence of collective charge behavior in the insulating state of ultrathin films of superconducting metals, Phys. Rev. Lett. **88**, 037004 (2002).

[24] H.-B. Jang, J. S. Lim, and C.-H. Yang, Film-thickness-driven superconductor to insulator transition in cuprate superconductors, Sci. Rep. **10**, 3236 (2020).

[25] Y. Yun, Y. Ma, T. Su, W. Xing, Y. Chen, Y. Yao, R. Cai, W. Yuan, and W. Han, Role of La doping for topological Hall effect in epitaxial EuO films, Phys. Rev. Mater. **2**, 034201 (2018).

[26] J. M. Riley, F. Caruso, C. Verdi, L. B. Duffy, M. D. Watson, L. Bawden, K. Volckaert, G. van der Laan, T. Hesjedal, M. Hoesch, F. Giustino, and P. D. C. King, Crossover from lattice to plasmonic polarons of a spin-polarised electron gas in ferromagnetic EuO, Nat. Commun. **9**, 2305 (2018).

[27] K. Epstein, A. M. Goldman, and A. M. Kadin, Vortex-antivortex pair dissociation in two-dimensional superconductors, Phys. Rev. Lett. **47**, 534 (1981).

[28] V. L. Berezinski, Destruction of long-range order in one-dimensional and two-dimensional systems possessing a continuous symmetry group. II. Quantum systems, Sov. J. Exp. Theor. Phys. **34**, 610 (1972).

[29] J. M. Kosterlitz and D. J. Thouless, Ordering, metastability and phase transitions in two-dimensional systems, J. Phys. C: Solid State Phys. **6**, 1181 (1973).

[30] M. R. Beasley, J. E. Mooij, and T. P. Orlando, Possibility of vortex-antivortex pair dissociation in two-dimensional superconductors, Phys. Rev. Lett. **42**, 1165 (1979).

[31] B. I. Halperin and D. R. Nelson, Resistive transition in superconducting films, J. Low Temp. Phys. **36**, 599 (1979).

[32] See Supplemental Material at http://link.aps.org/supplemental/10.1103/PhysRevB.109.054509 for Hall resistance R_{xy} vs B of sample A at $T = 10$ K; R_s vs T curve and the fitting curve based on the Halperin-Nelson formula.

[33] H. Matsuoka, M. Nakano, T. Shitaokoshi, T. Ouchi, Y. Wang, Y. Kashiwabara, S. Yoshida, K. Ishizaka, M. Kawasaki, Y. Kohama, T. Nojima, and Y. Iwasa, Angle dependence of H_{C2} with a crossover between the orbital and paramagnetic limits, Phys. Rev. Res. **2**, 012064(R) (2020).

[34] P. Baidya, D. Sahani, H. K. Kundu, S. Kaur, P. Tiwari, V. Bagwe, J. Jesudasan, A. Narayan, P. Raychaudhuri, and A. Bid, Transition from three- to two-dimensional Ising superconductivity in few-layer $NbSe_2$ by proximity effect from van der Waals heterostacking, Phys. Rev. B **104**, 174510 (2021).

[35] M. Tinkham, Effect of fluxoid quantization on transitions of superconducting films, Phys. Rev. **129**, 2413 (1963).